Syntheses and Reductions of *C*-Dimesitylboryl-1,2-dicarba-*closo*-dodecaboranes†

Jan Kahlert,[a] Lena Böhling,[a] Andreas Brockhinke,[a] Hans-Georg Stammler,[a] Beate Neumann,[a] Louis M. Rendina,[b] Paul J. Low,[c] Lothar Weber,*[,a] and Mark A. Fox*[,d]

[a] Fakultät für Chemie der Universität Bielefeld, 33615 Bielefeld, Germany.

E-mail: lothar.weber@uni-bielefeld.de

[b] School of Chemistry, The University of Sydney, Sydney, NSW 2006, Australia.

[c] School of Chemistry and Biochemistry, University of Western Australia, 35 Stirling Highway, Crawley, Perth 6009, Australia

[d] Department of Chemistry, Durham University, Durham DH1 3LE, United Kingdom.

E-mail: m.a.fox@durham.ac.uk

†*In memory of Ken Wade, a brilliant chemist and mentor.*

Abstract:

Two *C*-dimesitylboryl-1,2-dicarba-*closo*-dodecaboranes, 1-($BMes_2$)-2-R-1,2-$C_2B_{10}H_{10}$ (**1**, R = H, **2**, R = Ph), were synthesised by lithiation of 1,2-dicarba-*closo*-dodecaborane and 1-phenyl-1,2-dicarba-*closo*-dodecaborane, respectively, with *n*-butyllithium and subsequent reaction with fluorodimesitylborane. These novel compounds were structurally characterised by X-ray crystallography. UV absorption bands at 318-333 nm were observed for **1** and **2** corresponding to local π-π*-transitions within the dimesitylboryl groups while visible emissions at 541-664 nm with Stokes shifts of 11920-16170 cm^{-1} were attributed to intramolecular charge transfer transitions between the mesityl and cluster groups. Compound **2** was shown by cyclic voltammetry to form a stable dianion on reduction. NMR spectra for the dianion [**2**]$^{2-}$ were recorded from solutions generated by reductions of **2** with alkali metals and compared with NMR spectra from reductions of 1,2-diphenyl-*ortho*-carborane. On the basis of observed and computed ^{11}B NMR shifts, these *nido*-dianions contain bowl-shaped cluster geometries. The carborane is viewed as the electron-acceptor and the mesityl group is the electron-donor in *C*-dimesitylboryl-1,2-dicarba-*closo*-dodecaboranes.

Electronic supporting information: NMR data and spectra for **1**, **2** and dianions [**2**]$^{2-}$ and [**3**]$^{2-}$, absorption spectra for **1** and **2**, detailed CV data for **1** and **2**, computed GIAO-NMR and TD-DFT data for **1** and **2** and Cartesian coordinates for seven optimised geometries.

Introduction

Tri-coordinate boron compounds have been intensely investigated over the past two decades in view of potential applications as functional materials.[1] The most widely employed functional moiety containing a tri-coordinate boron atom is the dimesitylboryl group ($BMes_2$; Mes = 2,4,6-$Me_3C_6H_2$) in which the unsaturated boron centre is kinetically stabilised by steric shielding of the mesityl groups. The empty p_z-orbital at the boron atom can interact with the π-system of attached organic skeletons which leads to a narrowing of the HOMO-LUMO-gap (HLG) by lowering the LUMO energy. Therefore organic molecules containing $BMes_2$ units have been used as electron-transporting materials in opto-electronic devices.[2,3] The π-acceptor strength of the $BMes_2$ group is similar to those of cyano-[4] and nitro-[5] groups. Compounds with $BMes_2$ can be strongly fluorescent and thus have been used in organic light emitting diodes (OLEDs).[3,6] Moreover, the ability of the boron atom to form selectively covalent adducts with small anions has led to applications of these compounds as colorimetric and luminescent sensors for fluoride[7] and cyanide.[8]

Boron compounds that have gained considerable interest in the last seven years in the field of opto-electronic materials are derivatives of the dicarba-*closo*-dodecaborane isomers (1,2-, 1,7- and 1,12-$C_2B_{10}H_{12}$ which are *ortho*-, *meta*- and *para*-carborane, respectively).[9,10] Due to their delocalised systems (3D 'pseudoaromaticity'), these clusters possess high thermal and chemical stabilities.[11] The *ortho*-carborane is a unique electron-acceptor when connected to a donor at one or both cluster carbon atoms (at C1 and/or C2 in 1,2-$C_2B_{10}H_{12}$) due to the elasticity of the cluster C1-C2 bond.[12,13] The *ortho*-carborane unit thus can play an active role as the acceptor in the luminescence of donor-acceptor molecules (dyads). Photoexcitation of such dyads induce a charge transfer from an organic scaffold to the carborane cluster which either lead to luminescence quenching[14] or to charge transfer (CT) emissions (or both) depending on the solvents used[15-17] or as solids.[18-24]

Compounds with both $BMes_2$ and *ortho*-carboranyl groups are known[25] with *para*-phenylene bridges linking both units. In these systems, the *ortho*-carboranyl group is regarded as merely a strongly inductive electron-withdrawing group as the cluster increased the Lewis acidity of the triarylborane by fluoride ion titrations compared to the triarylborane without the cluster attached.

Of the few *ortho*-carboranes with tri-coordinate boron substituents at their carbon atoms reported,[20-22,26-28] only *C*-benzodiazaborolyl-*ortho*-carboranes were investigated regarding their photophysical, electrochemical and spectroelectrochemical properties.[21] However, the benzodiazaborolyl group generally acts as a π-donor and is therefore

electronically quite distinct from the $BMes_2$ moiety. In order to better understand the photophysical and electrochemical properties of *ortho*-carboranes with boryl groups, studies with compounds containing a tri-coordinate boron π-acceptor would be appealing and allow one to determine whether the *ortho*-carborane cluster remains as the active electron-withdrawing group. Therefore we present herein the syntheses and X-ray crystal structures of two *ortho*-carborane derivatives **1** and **2** with a $BMes_2$ group at one of the cage carbon atoms and their photophysical and electrochemical properties (Figure 1). The geometry of the reduced species of **2** was also determined by a combination of ^{11}B NMR spectroscopy and GIAO-NMR DFT computations.

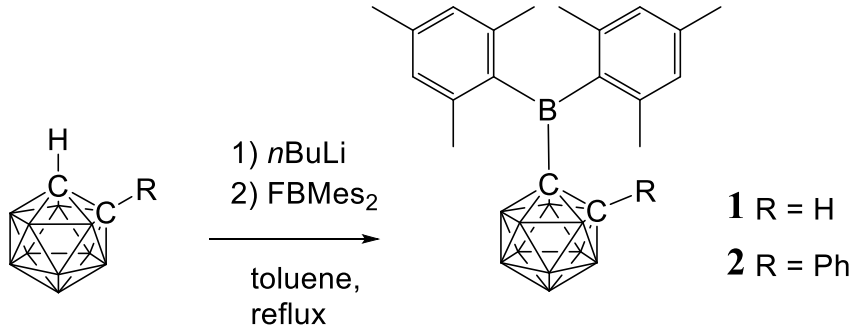

Figure 1. Syntheses of the novel *C*-dimesitylboryl-*ortho*-carboranes **1** and **2**.

Results and Discussion

Syntheses and characterisation of 1 and 2

Compounds **1** and **2** were synthesised by reaction of fluorodimesitylborane with the corresponding *C*-lithiocarborane, generated *in situ* by metallation of *ortho*-carborane and 1-phenyl-*ortho*-carborane, in boiling toluene (Figure 1). The elevated temperatures proved to be essential as no conversion was observed at ambient temperature. Purification was achieved by aqueous work-up and the target compounds were isolated in moderate yields by crystallization from *n*-hexane/dichloromethane mixtures. Although both compounds can be handled and stored in air for several hours, long-term storage is recommended under inert atmosphere as prolonged air contact led to changes in colour and shape of the crystals. In the case of **1,** decomposition of the B-C bond connecting the cluster and the $BMes_2$-unit has been observed presumably via hydrolysis.

Signals in the $^{11}B\{^1H\}$ NMR spectra of **1** and **2** between 3.7 and –12.9 ppm confirm the presence of the *ortho*-carborane clusters. The ^{11}B peaks at 78.9 ppm (**1**) and 80.4 ppm (**2**) are assigned to the $BMes_2$ groups and are very broad compared to the peaks corresponding to the cluster. The ^{11}B chemical shifts of the Mes_2B groups in **1** and **2** are virtually identical to

trimesitylborane (79.2 ppm) and phenyldimesitylborane (79.3 ppm).[29] Thus, the *ortho*-carboranyl groups influence the chemical shift of the three-coordinate boron atom of the $BMes_2$ unit in the same manner as a phenyl or mesityl substituent.

As many organic dimesitylboranes have been explored as fluoride sensors,[7,25] the reactivity of **1** and **2** towards fluoride ions was of interest. Chloroform solutions of **1** and **2** were treated with an excess of tetrabutylammonium fluoride trihydrate but only the parent carborane and dimesitylborinic acid[29] were detected by $^{11}B\{^1H\}$ NMR spectroscopy after fluoride addition. Control experiments confirmed that water alone does not lead to hydrolysis under these conditions.

X-ray crystallography

Single crystals of **1** and **2** were grown from *n*-hexane/dichloromethane mixtures and their molecular structures were determined by X-ray diffraction (Figure 2). The compounds crystallised in the orthorhombic space groups $Pna2_1$ (**1**) and $P2_12_12_1$ (**2**). Table 1 lists bond lengths and angles of interest with the atom labelling displayed in Figure 3.

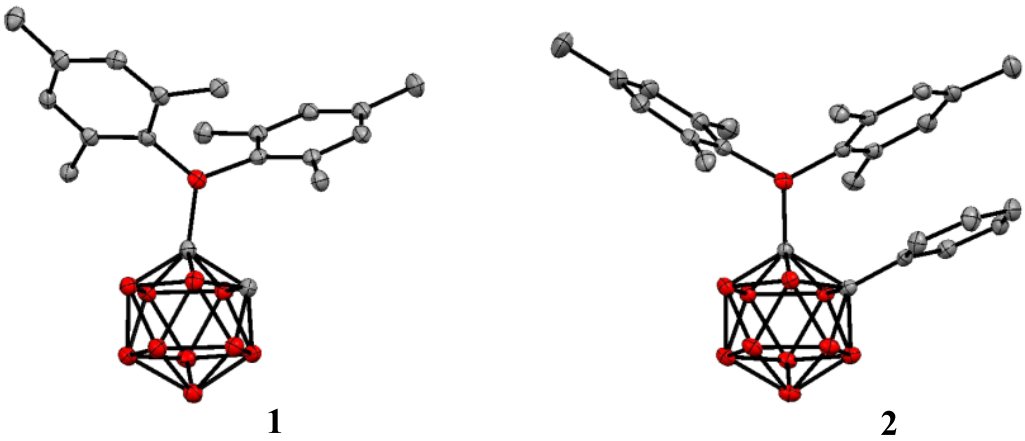

Figure 2. Molecular structures of **1** and **2** determined by X-ray crystallography. Hydrogen atoms are omitted for clarity.

The $BMes_2$ groups in **1** and **2** adopt orientations in which the empty p_z-orbitals of the boron atoms are at angles of 54.5° (**1**) and 67.7° (**2**) with respect to the C1-C2 bond of the cage (average of the torsion angles C2-C1-B1-C3/C12). Thus the p_z-orbitals are approximately in plane with the bonds C1-B3 in the clusters (averaged torsion angles B3-C1-B1-C3/C12: 12.5° (**1**), 5.7° (**2**)). These C1-B3 bonds are shorter than the bonds C1-B6 by 0.1 - 0.2 Å in both compounds. However, all B-B and B-C bonds lengths in the clusters are within the usual range.[20]

Table 1. Selected bond lengths and angles for **1** and **2**.

	1		**2**	
	exp.	calcd.	exp.	calcd.
Bond lengths [Å]				
C1-C2	1.677(3)	1.671	1.761(2)	1.791
C1-B1	1.635(3)	1.641	1.629(2)	1.648
C1-B3	1.728(3)	1.723	1.727(2)	1.724
C1-B6	1.756(3)	1.757	1.748(2)	1.751
B1-C3	1.595(3)	1.601	1.590(2)	1.597
B1-C12	1.581(3)	1.593	1.602(2)	1.602
Bond angles [°]				
C1-B1-C3	115.7(2)	116.9	118.2(1)	120.7
C1-B1-C12	121.0(2)	121.0	119.4(1)	118.3
C3-B1-C12	123.3(2)	122.2	122.4(1)	120.9
Torsion angles [°]				
C2-C1-B1-C3	36.0	34.9	22.5	37.1
C2-C1-B1-C12	–144.5	–145.1	–157.8	–145.8
B3-C1-B1-C3	102.7	102.1	95.8	110.6
B3-C1-B1-C12	–77.8	–77.8	–84.5	–72.3
Interplanar angles [°]				
(C1,B1,C3,C12)(C3 - C8)	77.9		78.6	
(C1,B1,C3,C12)(C12 - C17)	54.1		65.5	

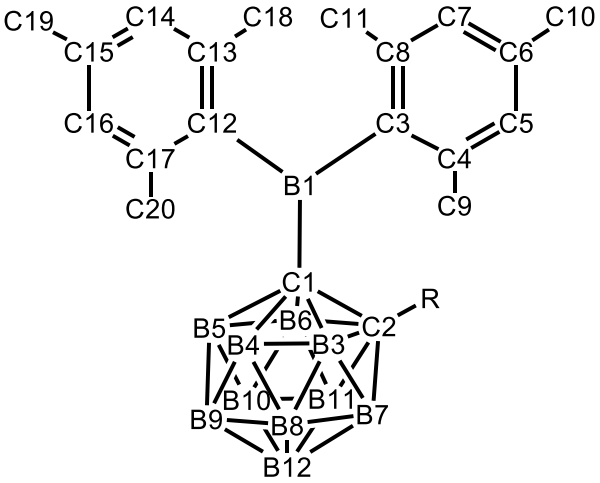

Figure 3. Atom labelling of *C*-dimesitylboryl-*ortho*-carboranes (R = H or Ph).

The C1-C2 distance of 1.677(3) Å in **1** agrees within 3 esd with the corresponding bond length of 1.670(1) Å for the carborane analogue bearing a 1,3-diethyl-1,3,2-benzodiazaborol-2-yl group in place of the $BMes_2$ unit.[20] Thus both monoboron groups exert similar effects on the cluster geometries in the observed conformations despite their different electronic properties. Similar C1-C2 bond lengths of 1.667(1)-1.673(1) Å are found in other

C-monoboryl-*ortho*-carboranes.[27,28] By contrast, the C1-C2 bond of 1.761(2) Å in **2** is significantly longer than in its 1,3-diethyl-1,3,2-benzodiazaborol-2-yl analogue (1.701(2) - 1.730(2) Å),[20] in 1,2-diphenyl-*ortho*-carborane (1.720(4)-1.733(4) Å)[30] and 1,2-diboryl-*ortho*-carboranes (1.695(1)-1.725(2) Å).[22,28] The longer C1-C2 bond in **2** is explained by the different steric interactions between the $BMes_2$ group at C1 and the phenyl ring at C2 in **2**.

The $BMes_2$ groups are linked to the cage carbon atoms by B-C single bonds (C1-B1) with lengths of 1.635(3) Å in **1** and 1.629(2) Å in **2**, which is at the upper edge of the range determined for other *C*-boryl-*ortho*-carboranes (1.607(4) - 1.649(12) Å).[20-22,27,28] The B-C bond lengths between the mesityl rings and the boryl-boron atoms (B1-C3/C12 1.581(3) Å - 1.602(2) Å) are typical for dimesitylboranes. As a consequence of the three-dimensional shape of the cluster in both structures, the interplanar angle enclosed by the mesityl ring pointing towards the second cage carbon atom and the plane defined by the boryl-boron atoms and the three neighbouring carbon atoms (77.9° (**1**), 78.6° (**2**)) is larger than in most reported structures of $BMes_2$ compounds.[31] A virtually perpendicular orientation of the phenyl substituent in **2** with respect to the C1-C2 axis (torsion angles = 94.3°, –91.5°) corresponds to the situation in other disubstituted phenyl-*ortho*-carboranes and is preferred due to sterics.[30,32]

Photophysics

Photophysical data for **1** and **2** are listed in Table 2. The absorption maxima of both *C*-dimesitylboryl-*ortho*-carboranes (Figure S11) in solvents of different polarity do not display any significant solvatochromism. The lack of solvatochromism points to very similar dipole moments in the electronic ground state and the initial excited state indicating that local transitions within the dimesitylboryl unit give rise to the absorption bands observed. The presence of the phenyl ring at C2 in **2** appears to lower the HOMO-LUMO energy gap as the absorption maxima of **2** (330 nm - 333 nm) are bathochromically shifted by approximately 12 - 14 nm compared to **1** (318 - 319 nm) in all solvents used. The energy difference in the absorption maxima between **1** (329 nm) and **2** (332 nm) in the solid state is smaller.

Emission maxima of both compounds in cyclohexane are virtually identical at 541 nm for **1** and 544 nm for **2** with large Stokes shifts of 12300 cm^{-1} for **1** and 11920 cm^{-1} for **2**. The luminescence spectra (Figure 4) reveal positive solvatochromism with emission maxima in the more polar solvent dichloromethane in the red emission region at 664 nm for **1** and 643 nm for **2**. By using the Lippert-Mataga method with an Onsager radius of 4.00 Å estimated from the molecular structures, the calculated transition dipole moments are 10.4 D (**1**) and 9.2 D (**2**) similar to transition dipole moments of *C*-benzodiazaborolyl-*ortho*-carboranes (6.9 -

10.9 D).[20-22] The results show that the carborane cluster plays a part in the emission process acting as the electron acceptor of the charge transfer process after excitation. The solid-state emissions occur at longer wavelengths than in cyclohexane (Figure 5). This bathochromic shift is more pronounced for **1** (567 nm) than for **2** (550 nm) and is presumably caused by fluorophor-fluorophor interactions. The quantum yields (Φ) are very low in all solvents (< 1%) with higher values of 2% (**1**) and 7% (**2**) found in the solid state.

In addition to these low-energy emissions, compound **1** displays a weaker emission band at the violet edge of the visible spectrum in polar solvents. The high-energy emissions with smaller Stokes shifts of 4710 - 6600 cm^{-1} probably originate from local transitions at the $BMes_2$ group.[33] Similar dual emissions originating from both local and CT transitions have been reported for some *ortho*-carboranes with substituents at one or both cluster carbon atoms.[16,20-23]

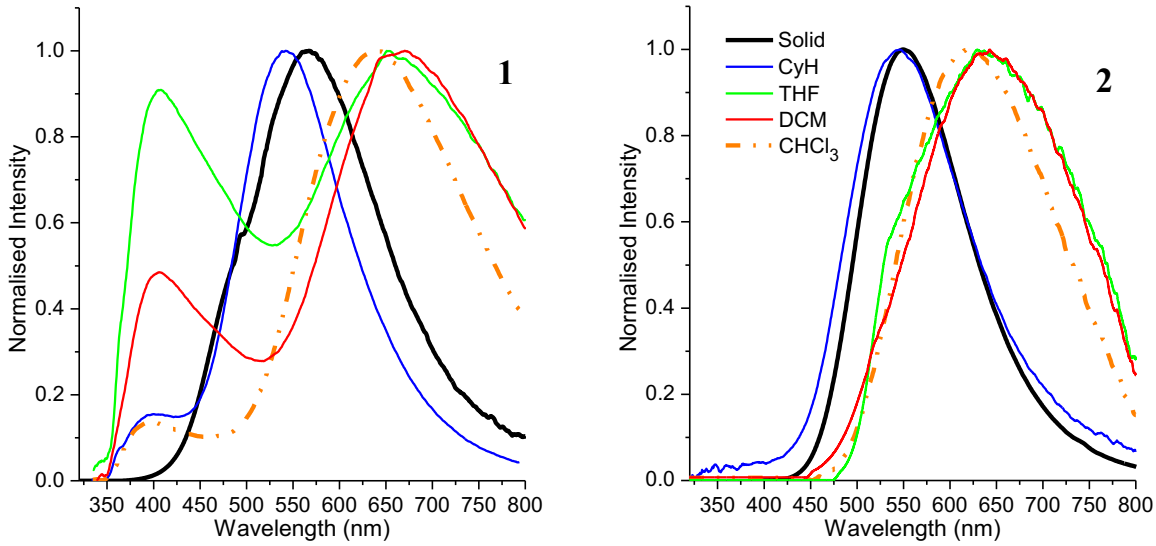

Figure 4. Emission spectra of **1** and **2** in the solid state and in various solvents.

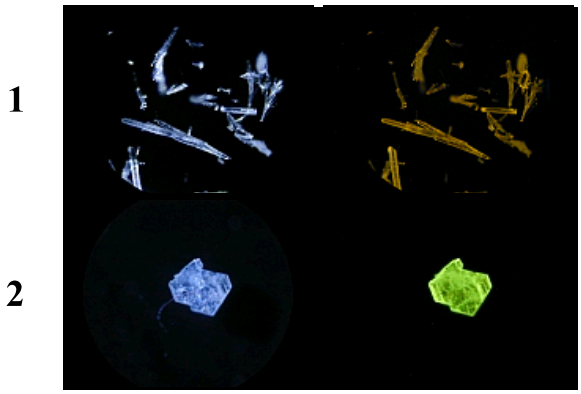

Figure 5. Crystals of **1** and **2**. Left column: Without UV irradiation. Right column: Under UV irradiation at 350 nm.

Table 2. Photophysical data for **1** and **2**.

		Solid	CyH	$CHCl_3$	THF	DCM
Absorption λ_{max} [nm] (ε)[a]	**1**	329	318 (8300)	319 (7350)	319 (7060)	318 (7920)
	2	332	332 (6750)	331 (7330)	333 (5710)	330 (7760)
Emission λ_{max} [nm] (relative height)	**1**	567	400, 541 (0.15 : 1)	396, 641 (0.14 : 1)	408, 653 (0.91 : 1)	406, 664 (0.48 : 1)
	2	550	544	620	640	643
Stokes shift [cm^{-1}]	**1**	12310	5500, 12300	5780, 15610	6240, 15600	6600, 16170
	2	9210	11920	14310	14660	14800

[a] in L mol^{-1} cm^{-1}.

Electrochemistry

The electrochemical properties of both *C*-dimesitylboryl-*ortho*-carboranes **1** and **2** were investigated by cyclic voltammetry (CV, Figure 6). The peak potentials measured in acetonitrile and dichloromethane solutions, with platinum and glassy carbon working electrodes are listed in Table S4. The traces resemble reported CV data on reductions of carboranes[16,17,21-23,34-39] and thus reductions take place at the carborane clusters in **1** and **2**. CV traces for reductions of the $BMes_2$ group would involve a simple one-electron reversible wave. For example, compound $PhBMes_2$ has a one-electron reversible wave at -2.30 V (vs the ferrocenium/ferrocene couple at 0.0 V).[4]

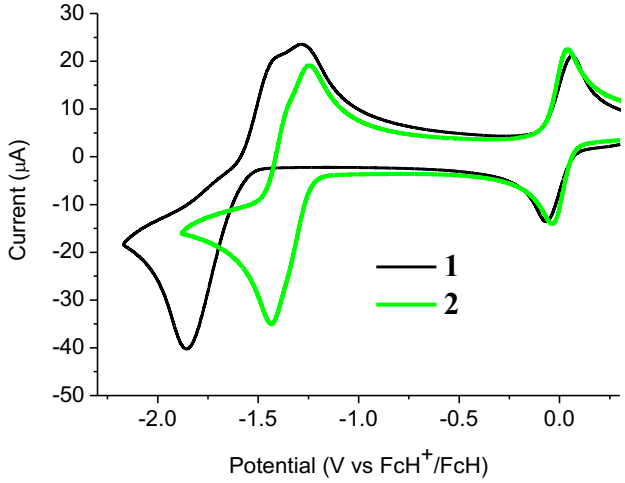

Figure 6: Cyclic voltammograms of **1** and **2** with a glassy carbon working electrode in acetonitrile and internal ferrocenium/ferrocene couples at 0.0 V.

A CV trace for *ortho*-carborane or a C-monosubstituted-*ortho*-carborane usually shows a two-electron cathodic wave and an anodic wave that is not of the same current intensity as the cathodic wave.[21,34,35] Often the peak-peak separation between the two waves can be several hundred millivolts due to the structural rearrangement of the dianion on the CV timescale. Decomposition processes can also complicate the electrochemical response. One possible decomposition pathway from the dianion is that cage C-H cleavage takes place resulting in a *closo*-carborane anion and a hydride ion. Alternatively, the monoanion initially formed gives a *closo*-carborane anion and a hydrogen radical.[40] Another pathway is that the dianion formed is readily protonated, giving rise to a proton-coupled electron transfer (PCET) response.[34]

The CV of **1** in acetonitrile with a glassy carbon working electrode shows a two-electron cathodic wave at -1.85 V and two anodic waves at -1.40 V and -1.28 V with values referenced to the ferrocenium/ferrocene redox couple at 0 V (Figure 6). The cathodic wave value of -1.85 V for **1** means that **1** is more easily reduced than C-monophenyl-*ortho*-carborane at -2.25 V[35] reflecting the substantial electron-withdrawing effect of the $BMes_2$ group. Similar CV traces are observed for **1** with a platinum working electrode and with DCM as solvent (Figure S9 and Table S4). The non-equivalent current intensities between the forward and reverse waves for **1** suggest that the dianion of $[\mathbf{1}]^{2-}$ is not stable and would be difficult to isolate.

A CV trace for *ortho*-carborane with aryl substituents at both cluster carbon atoms generally shows a reversible wave (or two) on reduction.[16,21-23,34,36-39] In several cases, a stepwise reduction involving two separated one-electron reduction steps has been found, with the initial reduction process giving rise to a radical anion with an unusual 2n+3 skeletal electron (SE) count. One example is diphenyl-*ortho*-carborane **3** where the radical anion has been shown to be stable enough to be observed spectroscopically (Figure 7).[36] The first one-electron reduction process on the CV timescale is usually slow due to the rearrangement of the cluster and is often immediately followed by a second one-electron process giving a cathodic two-electron wave. The latter wave is usually evident in DCM for these carboranes.[22] However, on back oxidation two separate anodic waves (with the combined current intensities similar to the current intensity of the cathodic wave) are evident corresponding to two one-electron processes.[21,22]

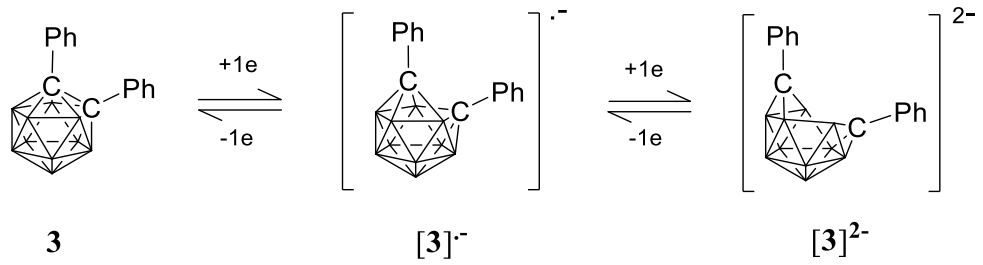

3 $[\mathbf{3}]^{\cdot-}$ $[\mathbf{3}]^{2-}$

Figure 7. Two one-electron reductions for 1,2-diphenyl-*ortho*-carborane **3**.

The CV of **2** in acetonitrile shows two one-electron waves in both directions with both waves very close together (Figure 6). These waves are separated by less than 80 mV based on gaussian analyses of its square-wave potential traces.(Figure S10) The two half-wave potentials are estimated to be -1.31 and -1.39 V which indicate that **2** is reduced more readily than diphenyl-*ortho*-carborane **3** at -1.57 and -1.72 V under the same CV conditions. Compound **2** does form a radical anion with a 2n+3 skeletal electron count but this is very unlikely to be isolated or even identified from spectra obtained by careful spectroelectrochemical experiments on **2**. The CV of **2** in DCM shows the expected CV pattern with a one two-electron cathodic wave and two one-electron anodic waves (Figure S9 and Table S4).

Strong electron-withdrawing substituents such as fluoroaryl groups[37] and bulky groups such as *tert*-butyl groups[21] can facilitate the formation of stable radical monoanions. The combined bulk and electron-withdrawing properties of the Mes_2B group did not improve the stability of the carborane radical monoanion with respect to the neutral and dianion species.

Computations

Calculated bond lengths and angles from geometries of **1** and **2** optimised at B3LYP/6-31G* are in good agreement with the experimental values (Table 1). The lengthening of the C1-B6 bonds compared to the C1-B3 bonds is attributed to steric repulsion between an *ortho*-methyl group of one of the mesityl rings and the B6-H unit. Computed energy barriers for the rotation around the C1-B1 bonds are 6.1 kcal·mol^{-1} in **1** and 18.6 kcal·mol^{-1} in **2**. Comparison between computed GIAO-NMR and experimental ^{11}B NMR chemical shifts for **1** and **2** are in very good agreement (Table S5).

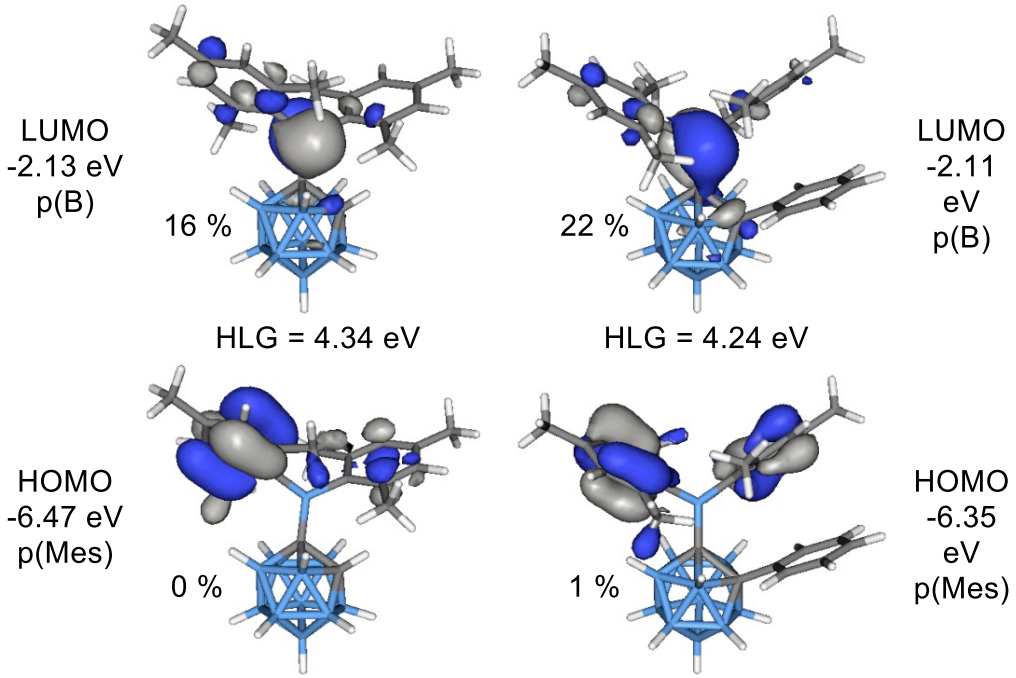

Figure 8: Frontier molecular orbitals of **1** (left) and **2** (right). The percentage values are the cluster contributions to the molecular orbitals.

Figure 8 shows the frontier molecular orbitals of both compounds. The HOMO is a combination of π-orbitals at the mesityl groups (π(Mes)) and the LUMO consists mainly of the empty p-orbital of the boryl boron atom (p(B)). Antibonding orbitals with significant cluster contributions have much higher energies (> -0.16 eV) and thus the influence of the clusters on the absorption process is merely inductive in both cases. According to TD-DFT calculations π(Mes)-p(B) transitions with oscillator strengths (*f*) of 0.0065 to 0.0698 can be assigned to the absorption bands of both compounds (Tables S6 and S7). Therefore, the electron density in the initially formed excited state is localised within the $BMes_2$-unit and is not expected to entail strong changes in the overall dipole moment. This is in agreement with the lack of solvatochromism in the absorption spectra. Weak transitions between the π-orbitals of the phenyl group of **2** and the p(B) orbital as well as π-π* transitions within the phenyl ring occur at considerably higher energy far in the UV region. The HOMO-LUMO gap energy of **2** is 0.10 eV smaller than that in **1** which agrees well with the observed bathochromic shift of the absorption maximum of **2** compared to **1**.

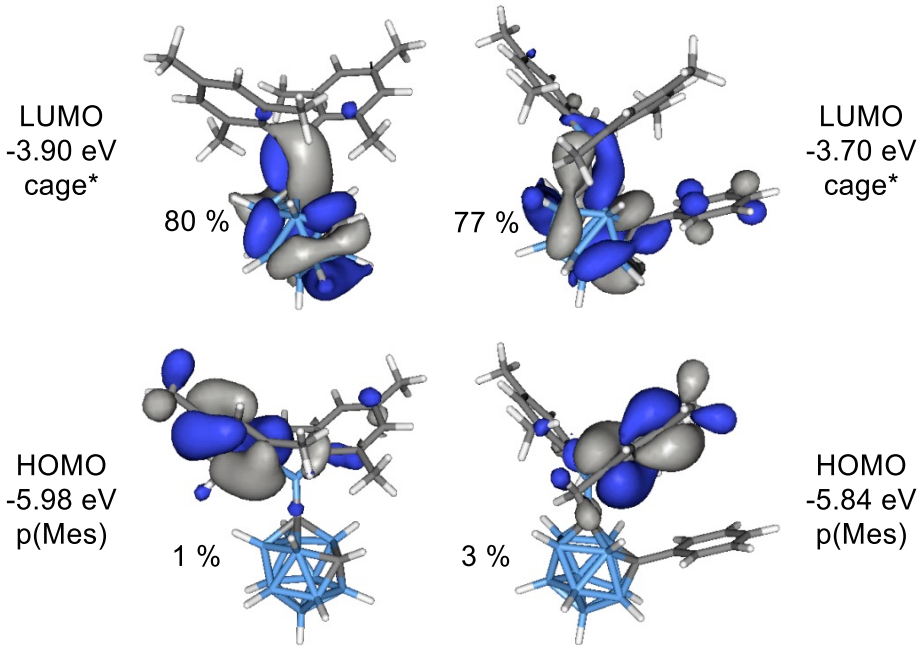

Figure 9: Frontier orbitals of the S_1 geometries of **1** (left) and **2** (right). The percentage values are the cluster contributions to the molecular orbitals.

In order to elucidate the origin of the visible CT emission of **1** and **2**, their geometries were optimised at the first excited singlet state (S_1). In both cases "open" cluster geometries were found with C1-C2 distances expanded to 2.384 Å (**1**) and 2.440 (**2**), respectively. The frontier orbitals of the S_1 geometries are depicted in Figure 9. These orbitals were calculated at the ground state, S_0 thus HOMO and LUMO correspond to the highest and second highest singly occupied orbitals in the S_1 state. The HOMO is a π(Mes) orbital but the LUMO, in contrast, is an antibonding cluster orbital (cage*) with small contributions from the exopolyhedral boron atom (**1**: 15%, **2**: 8%). Thus, the HOMO-LUMO transition corresponds to a charge transfer between the cluster and the mesityl groups from the excited state and the two compounds can be regarded as donor-acceptor systems. TD-DFT calculations predicted low-energy emissions with low oscillator strengths at 859 nm (**1**; f = 0.0016) and 783 nm (**2**; f = 0.0066) for these transitions and gave the same trend as experimentally observed with **1** emitting at longer wavelength than **2**.

Geometries of the dianions $[2]^{2-}$ and $[3]^{2-}$

While *closo*-dicarbadodecaboranes all adopt the pseudo-icosahedral geometry, several different geometries of *nido*-dicarbadodecaborane dianions have been determined crystallographically (Figure 10).[41] Dianions with almost planar C_2B_4 open faces like $[\mathbf{4}]^{2-}$ and

[**5**]$^{2-}$ are observed in Group 1 metallacarboranes.[42-45] Some C_2B_4 open-face dianions may be regarded as 13-vertex monoanions where the alkali metal atom occupies the open face and acts as a thirteenth vertex typically found in many 13-vertex metallacarboranes[9] whereas some dianions may be considered to be discrete carborane dianions where the alkali metal atom(s) cap a triangular face instead.[42] Bowl-shaped geometries have been observed in carborane dianions like [**6**]$^{2-}$ and [**7**]$^{2-}$ with tethers at both cage carbons.[44,46] The crystal structures of sodium salts containing these tethered dianions all show the sodium atoms capping the triangular faces of the dianions rather than on the open faces. The bowl geometry in [**7**]$^{2-}$ differs from that in [**6**]$^{2-}$ where [**7**]$^{2-}$ has a notably smaller open face.[46] These bowl-shaped geometries are similar to geometries determined for neutral 12-vertex tetracarbadodecaboranes by X-ray crystallography.[47] The neutral compound **8** may also be regarded as a genuine 12-vertex dicarbadodecaborane dianion $[R_2C_2B_{10}H_{10}]^{2-}$ with two positively charged phosphonium groups.[48]

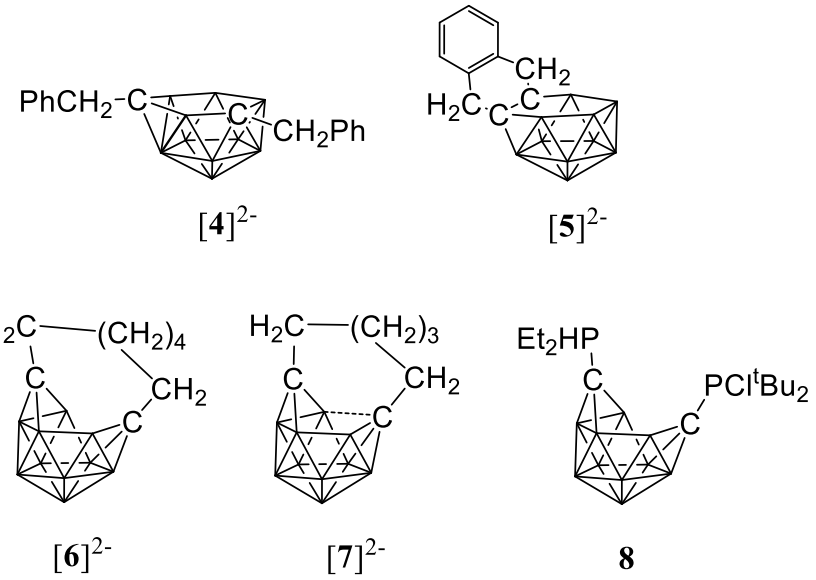

Figure 10. Geometries of *nido*-dicarbadodecaboranes determined by X-ray crystallography.

While there are several structural studies published on *nido*-dicarbadodecaborane dianions, the geometries of *nido*-dicarbadodecaborane dianions in solutions have not been determined. The successful method[49] of comparing observed and computed ^{11}B NMR data to determine carborane cluster geometries is applied here for dianion [**2**]$^{2-}$. Before discussing the dianion [**2**]$^{2-}$made by chemical reductions on **2**, the dianion [**3**]$^{2-}$ generated from diphenyl-*ortho*-carborane **3** is described here to demonstrate the use of the combined experimental and calculated ^{11}B NMR method in determining the geometry of its dianion. Dianion [**3**]$^{2-}$ has been proposed to have a geometry[50] with a C_2B_4 open face **A** or a geometry[39,51] with a C_2B_2

open face **B** (Figure 11). Thus, the geometry of the dianion [**3**]$^{2-}$ has not been established even though this dianion has been known for many decades. [52]

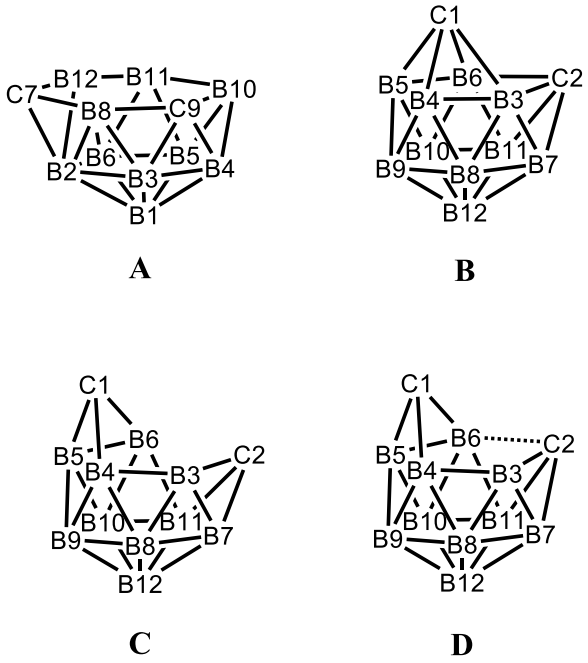

Figure 11. Geometries **A**-**D** of *nido*-dicarbadodecaborane dianions with atom numbering.

Chemical reductions of **3** were carried out with alkali metals (Li, Na, K) in THF solutions. The THF reactions were monitored by ^{11}B NMR spectroscopy until all the peaks corresponding to the starting carborane and the red colours of the solutions due to the radical monoanions disappeared. The ^{11}B{^{1}H} spectra of the dianions [**3**]$^{2-}$ in clear yellow solutions show 2:2:4:2 patterns which are not significantly influenced by the different alkali metal cations (Figure 12). This pattern suggests a geometry of high symmetry or two mirror-image geometries that are fluctional in solution for [**3**]$^{2-}$ with the metal cations not strongly interacting in solution.

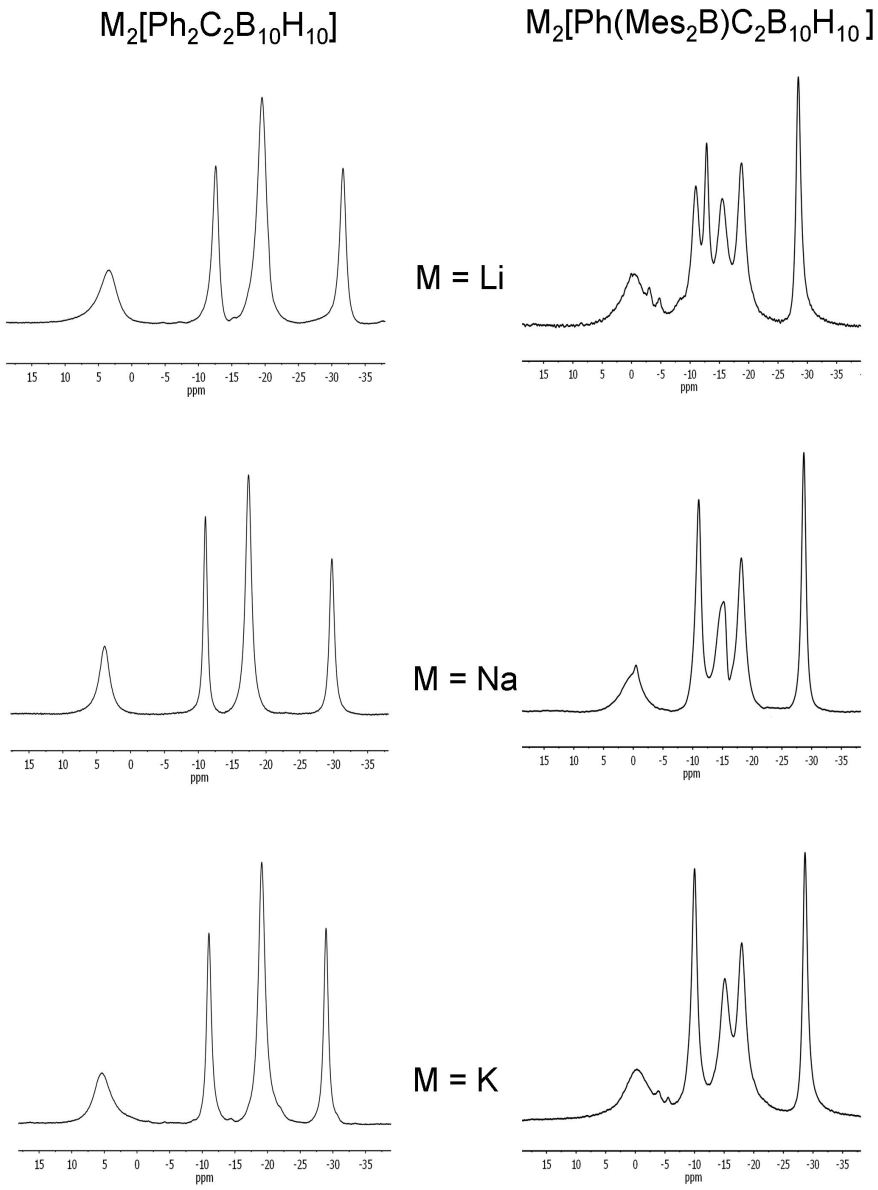

Figure 12: $^{11}B\{^{1}H\}$ NMR spectra of $M_2[\mathbf{3}]^{2-}$ and $M_2[\mathbf{2}]^{2-}$ (M = Li, Na or K) in THF. The broad peaks at 65-70 ppm corresponding to the boryl boron in $[\mathbf{2}]^{2-}$ are not shown here.

Geometry optimisations on $[\mathbf{3}]^{2-}$ reveal that the bowl-shaped geometry **C** is more stable than **A** and **B** by 5.5 and 11.0 kcalmol^{-1} respectively. More importantly, the computed GIAO ^{11}B NMR chemical shifts of the bowl-shaped geometry fit well with observed shifts when fluctionality between the two mirror-image geometries of **C** takes place in solution (Table 3). The geometry **D** found in $[\mathbf{7}]^{2-}$ could not be located for $[\mathbf{3}]^{2-}$ where the initial geometry **D** rearranged to **C** on optimisation.

Table 3: Computed and observed $^{11}B\{^1H\}$ NMR data of $[\mathbf{2}]^{2-}$ and $[\mathbf{3}]^{2-}$ in ppm and relative energies of the optimised geometries in kcalmol^{-1}.

	Geometry	B3,6	B12	B9	B4,5	B7,11	B8,10	$BMes_2$	Rel. E
$[\mathbf{2}]^{2-}$	**A**[a]								14.0
	C	13.3	-1.2	-8.4	-17.4	-21.3	-23.7	60.2	0.0
	D	–4.1	–10.5	–11.8	–15.4	–19.5	–29.2	56.0	0.8
Exp.[b]		0.1	–9.2	–10.1	–14.0	–17.8	–27.2	67.5	
$[\mathbf{3}]^{2-}$	**A**[c]								11.0
	B	-23.5	-20.0	-20.0	-18.6	-18.6	-55.7		5.5
	C	12.2	-7.6	-7.6	-20.7	-20.7	-25.5		0.0
Exp.[d]		7.0	-9.3	-9.3	-17.3	-17.3	-27.5		

[a] All borons are non-equivalent in geometry **A** of $[\mathbf{2}]^{2-}$, values are calculated assuming same fluctionality process as in geometry **A** of $[\mathbf{3}]^{2-}$; 64.6 ($BMes_2$), 14.1 (B12), 12.1 (B10), 5.7 (B11), -0.7 (B4), -1.7 (B6), -7.3 (B8), -18.2 (B5), -20.3 (B1), -23.9 (B3), -24.8 (B2).
[b] Experimental data for sodium salt in CD_3CN, Figure 12.
[c] Calculated values are averaged assuming fluctionality between two mirror-image geometries; 10.0 (B10,12), -0.8 (B11), -6.0 (B8), -9.3 (B5,6), -18.8 (B3), -20.6 (B2,4), -25.6 (B1).
[d] Experimental data for sodium salt in d_8-THF.

Reduction of **2** with sodium metal in 1,2-dimethoxyethane (DME) yielded a dark red solid identified as $[Na(DME)_n]_2[\mathbf{2}]$ by ^1H, ^{11}B and ^{13}C NMR spectroscopy. The $^{11}B\{^1H\}$ NMR spectrum recorded in CD_3CN revealed a 2:1:1:4:2 pattern for the cluster atoms and a very broad signal at 67.5 ppm corresponding to the boryl boron atom (Figure 13). The latter peak is considerably shifted to higher field by about 13 ppm compared to the neutral starting material. Chemical reductions of the Mes_2B compound **2** in THF with alkali metals were carried out as for **3**. After observation of the purple colours corresponding to the radical species and the disappearance of the peaks corresponding to the starting material, the clear solutions containing the dianions $[\mathbf{2}]^{2-}$ were dark red. ^{11}B NMR spectra of the dianions $[\mathbf{2}]^{2-}$ show either a 2:1:1:2:2:2 (Li salt) or a 2:2:2:2:2 (Na, K) peak pattern (Figure 12) and are similar to peaks found for the diphenylcarborane dianions $[\mathbf{3}]^{2-}$ when taking into account the lower symmetry in $[\mathbf{2}]^{2-}$.

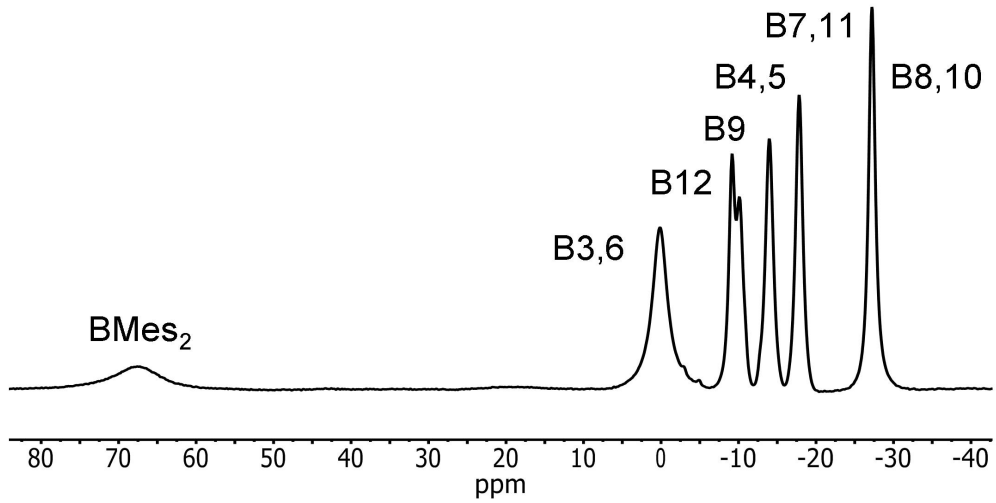

Figure 13: $^{11}B\{^{1}H\}$ NMR spectrum of $[\mathbf{2}]^{2-}$ in CD_3CN with peak assignments based on GIAO-NMR data.

The similarities in the ^{11}B NMR peaks observed for $[\mathbf{2}]^{2-}$ and $[\mathbf{3}]^{2-}$ suggest that both have bowl-shaped geometries. Geometry optimisations on the $BMes_2$ species $[\mathbf{2}]^{2-}$ reveal that the starting geometry **B** was rearranged to the bowl-shaped geometry **D**. The most stable geometry for $[\mathbf{2}]^{2-}$ is **C** with **D** only 0.8 kcalmol^{-1} higher in energy. However, computed ^{11}B NMR shifts from geometry **D** fit better with observed ^{11}B NMR shifts than geometry **C** for $[\mathbf{2}]^{2-}$ assuming fluxionalities between mirror-image geometries occur in solution (Figure 14).

It is concluded here that bowl-shaped geometries are present in solutions of 12-vertex *nido*-dicarbadodecaborane dianions with fluctional cluster geometries of **C** and **D** in dianions of *C*,*C'*-diphenyl-carborane $[\mathbf{3}]^{2-}$ and *C*-dimesitylboryl-*C'*-phenyl-carborane $[\mathbf{2}]^{2-}$ respectively. The calculated geometries for $[\mathbf{2}]^{2-}$ and $[\mathbf{3}]^{2-}$ are similar to the experimental cluster geometries of $[\mathbf{7}]^{2-}$ and $[\mathbf{6}]^{2-}$ respectively as shown from comparison of distances involving the cluster carbon atoms, C1 and C2, in Table 4. The combined experimental and calculated ^{11}B NMR method is shown to be useful in determining *nido*-12-vertex geometries in solutions and will aid further progress on the intriguing range of *nido*-12-vertex geometries in the future.

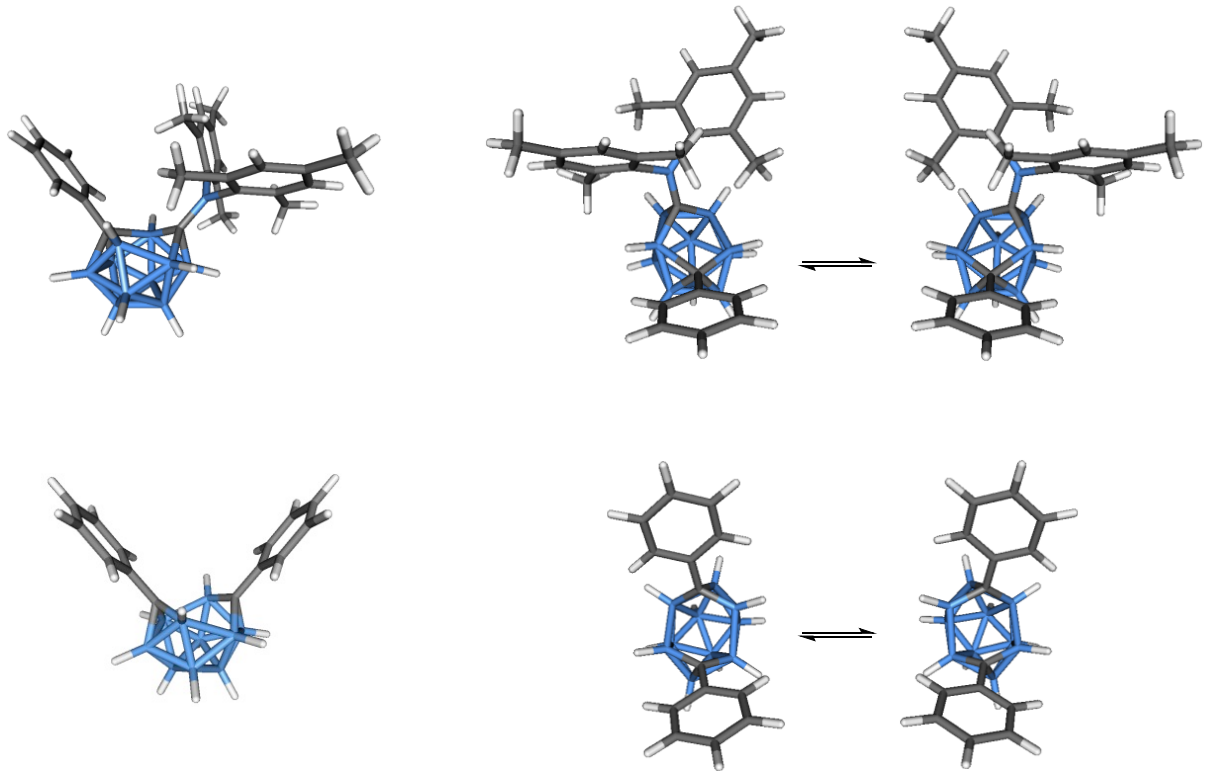

Figure 14: Optimised geometries of [**2**]$^{2-}$ (top) and [**3**]$^{2-}$ (bottom) and the fluxional processes.

Table 4. Comparison of selected distances in Å for the *nido*-dianions, [**2**]$^{2-}$, [**3**]$^{2-}$, [**6**]$^{2-}$ and [**7**]$^{2-}$.

	[**2**]$^{2-}$ calc.	[**7**]$^{2-}$ obs.	[**3**]$^{2-}$ calc.	[**6**]$^{2-}$ obs
C1…C2	2.666	2.687(6)	2.915	2.87(1)
C1…B3	2.528	2.302(9)	2.606	2.59(1)
C1…B6	1.624	1.617(9)	1.546	1.51(1)
C2…B3	1.586	1.534(8)	1.546	1.51(1)
C2…B6	1.878	2.083(8)	2.606	2.55(1)

Conclusions

Two *C*-dimesitylboryl-1,2-dicarba-*closo*-dodecaboranes were synthesised from fluorodimesitylborane and the corresponding lithio-carboranes and structurally characterised by X-ray crystallography. Photophysical studies and TD-DFT calculations showed that the absorptions correspond to local transitions within the $BMes_2$ groups whereas visible emissions with Stokes shifts up to 16170 and 14800 cm^{-1} in dichloromethane originate from intramolecular CT transitions between the mesityl rings and the cluster. Compound **2** with a phenyl substituent at the second cage carbon atom can be easily reduced to a stable dianion [**2**]$^{2-}$ by cyclic voltammetry and chemical reductions with alkali metals. Based on experimental and calculated ^{11}B NMR data, a dynamic bowl-shaped *nido*-cage geometry is

determined for the dianion. These findings indicate that the *ortho*-carboranyl group is a stronger electron acceptor than the $BMes_2$ group and *C*-dimesitylboryl-1,2-dicarba-*closo*-dodecaboranes are dyads with the mesityl group as the donor and the carborane as the acceptor.

Experimental Section

General: The reactions were performed under an atmosphere of dry oxygen-free argon using Schlenk techniques. All solvents were dried by standard methods and freshly distilled prior to use. Fluorodimesitylborane[53] and 1-phenyl-1,2-dicarba-*closo*-dodecaborane[54] were prepared as described in the literature. 1,2-Dicarba-*closo*-dodecaborane was purchased commercially (KatChem). NMR spectra were recorded from solutions at room temperature on a Bruker AM Avance DRX500 (^1H, ^{11}B, ^{13}C), a Bruker Avance III 500 and a Bruker Avance 400 Spectrometer ($^1H\{^{11}B\}$) with $SiMe_4$ (^1H, ^{13}C) and $BF_3{\cdot}OEt_2$ (^{11}B) as external standards. ^1H- and $^{13}C\{^1H\}$ NMR spectra were calibrated on the solvent signal [$CDCl_3$: 7.24 (^1H), 77.16 (^{13}C); CD_3CN: 1.94 (^1H), 118.25, 1.32 (^{13}C); d_8-THF: 3.58, 1.73 (^1H), 67.57, 25.46 (^{13}C)]. The ^{13}C NMR peaks were assigned with the aid of observed ^{13}C DEPT spectra and computed ^{13}C NMR shifts. Mass spectra were recorded with a VG Autospec sector field mass spectrometer (Micromass).

1-Dimesitylboryl-1,2-dicarba-*closo*-dodecaborane (1):

A solution of *n*-butyllithium (1.6 M in *n*-hexane, 2.37 mL, 3.79 mmol) was added to 1,2-dicarba-*closo*-dodecaborane (0.52 g, 3.61 mmol) in toluene (35 mL) at 0 °C. After 16 h stirring at ambient temperature a solution of fluorodimesitylborane (0.96 g, 3.58 mmol) in toluene (6 mL) was added to the resulting suspension. The mixture was heated at reflux temperature for 5 h and washed with water (2 × 10 mL) and saturated sodium chloride solution (10 mL) subsequently. The combined aqueous layers were extracted with toluene (10 mL) and the combined organic phases were dried over sodium sulfate and freed from volatiles *in vacuo*. The crude product was recrystallized from a mixture of *n*-hexane (30 mL) and dichloromethane (2 mL) to afford pure **1** as colourless crystals. Yield: 0.85 g (61 %). Found: C, 60.42; H, 8.51; N, 0.00 %; $C_{20}H_{33}B_{11}$ requires C, 61.22; H, 8.48; N, 0.00 %; ^1H-NMR ($CDCl_3$): δ [ppm] = 1.4 - 3.2 (m, br, 10 H, BH), 2.24 (s, 6 H, *para*-CH_3), 2.40 (s, 12 H, *ortho*-CH_3), 3.85 (s, br, 1 H, $B_{10}H_{10}C_2\underline{H}$), 6.80 (s, 4 H, CH_{Mes}); $^{13}C\{^1H\}$-NMR ($CDCl_3$): δ [ppm] = 20.9 (s, *para*-CH_3), 25.9 (s, *ortho*-CH_3), 61.6 (s, $CB_{10}H_{10}\underline{C}H$), 75.4 (s, $CB_{10}H_{10}\underline{C}BMes_2$), 129.7 (s, CH_{Mes}), 138.4 (s, C_{ipso}), 139.4 (s, $C_{ortho,}$), 139.8 (s, C_{para}); $^{11}B\{^1H\}$-NMR ($CDCl_3$): δ

[ppm] = –12.9 (s), –9.1 (s), –6.9 (s), –2.3 (s), 1.9 (s) (skeletal boron atoms), 78.9 (s, br, exopolyhedral boron atom) see Figures S1-S3 for NMR spectra of **1**; MS (EI): m/z = 392.4 (M^+, 3 %), 272.3 (M^+–HMes, 51 %), 249.2 ($BMes_2^+$, 46 %), 120.1 (Mes^+, 100 %).

1-Dimesitylboryl-2-phenyl-1,2-dicarba-*closo*-dodecaborane (2):

A solution of *n*-butyllithium (1.6 M in *n*-hexane, 3.10 mL, 4.96 mmol) was added to 1-phenyl-1,2-dicarba-*closo*-dodecaborane (0.97 g, 4.40 mL) in toluene (40 mL). After stirring for 16 h at ambient temperature a solution of fluorodimesitylborane (1.30 g, 4.85 mmol) in toluene (12 mL) was added and the mixture was heated at reflux temperature for 5 h. Subsequently it was washed with water (2 × 15 mL) and saturated sodium chloride solution (15 mL). The combined organic phases were dried over sodium sulfate and the solvent was removed *in vacuo*. Impurities were sublimed from the residue at 80 °C *in vacuo* and the remaining solid was recrystallized from a mixture of *n*-hexane (80 mL) and dichloromethane (5 mL). The product **2** was obtained as colourless crystals. Yield: 0.97 g (51 %). Found: C, 66.38; H, 7.97; N, 0.00 %; $C_{26}H_{37}B_{11}$ requires C, 66.66; H, 7.96; N, 0.00 %; ^{1}H NMR ($CDCl_3$): δ [ppm] = 1.5 - 4.2 (m, br, 10 H, BH), 2.16 (s, 6 H, *para*-CH_3), 2.26 (s, 12 H, *ortho*-CH_3), 6.56 (s, 4 H, CH_{Mes}), 6.87 (dd, $^3J_{HH}$ = 7.4 Hz, $^3J_{HH}$ = 7.6 Hz, 2 H, H_{meta}), 7.13 (t, $^3J_{HH}$ = 7.4 Hz, 1 H, H_{para}), 7.18 (d, $^3J_{HH}$ = 7.6 Hz, 2 H, H_{ortho}); ^{13}C{^{1}H} NMR ($CDCl_3$): δ [ppm] = 20.8 (s, *para*-CH_3), 26.8 (s, *ortho*-CH_3), 86.5 (s, $CB_{10}H_{10}\underline{C}Ph$), 87.3 (s, $CB_{10}H_{10}\underline{C}BMes_2$), 127.7 (s, $C_{meta,\ Ph}$), 129.3 (s, $C_{para,\ Ph}$), 129.4 (s, CH_{Mes}), 130.3 (s, $C_{ortho,\ Ph}$), 131.7 (s, $C_{ipso,\ Ph}$), 138.8 (s, $C_{ipso,\ Mes}$), 139.1 (s, $C_{para,\ Mes}$), 139.4 (s, $C_{ortho,\ Mes}$); ^{11}B{^{1}H} NMR ($CDCl_3$): δ [ppm] = –9.9 (s), –8.0 (s), –2.8 (s), 3.7 (s) (skeletal boron atoms), 80.4 (s, br, exopolyhedral boron atom) see Figures S4-S6 for NMR spectra of **2**; MS (EI): m/z = 468.4 (M^+, 4 %), 453.4 (M^+–Me, 2 %), 348.3 (M^+–HMes, 100 %), 332.3 (M^+–Me–Mes, 13 %), 249.2 ($BMes_2^+$, 85 %).

Reductions of 2 and 3

Method 1: A piece of excess sodium metal was added to a solution of 1-dimesitylboryl-2-phenyl-1,2-dicarba-*closo*-dodecaborane **2** (0.07 g, 0.14 mmol) in 1,2-dimethoxyethane (0.5 mL). A dark red colour occurred immediately on the surface of the metal. The mixture was sonicated for 1 h and filtered subsequently. The filtrate was freed from volatiles *in vacuo* and the dark red remainder was taken up in d_3-acetonitrile and analysed by NMR spectroscopy. ^{1}H NMR (CD_3CN): δ [ppm] = –0.4 - 3.0 (m, br, 10 H, BH), 2.15 (s, 6 H, *para*-CH_3), 2.32 (s, 12 H, *ortho*-CH_3), 6.52 (s, br, 4 H, CH_{Mes}), 6.76 (s, br, 1 H, H_{para}), 6.92 (s, br, 2 H, H_{Ph}), 7.43 (s, br, 2 H, H_{Ph}); ^{13}C{^{1}H} NMR (CD_3CN): δ [ppm] = 20.8 (s, *para*-CH_3), 25.1 (s, *ortho*-CH_3),

70.5 (s, $CB_{10}H_{10}\underline{C}Ph$), 106.7 (s, $CB_{10}H_{10}\underline{C}BMes_2$), 122.0 (s, CH_{Ph} *para*), 127.6 (br s, CH_{Mes}, CH_{Ph} *meta*), 128.7 (s, CH_{Ph} *ortho*), 133.6 (s, s, C_{Mes}-*para*), 140.9 (s, C_{Mes}-*ortho*), 149.4 (s, C_{Mes}-*ipso*), 154.2 (s, C_{Ph} *ipso*); $^{11}B\{^1H\}$ NMR (CD_3CN): δ [ppm] = –27.2 (s), –17.8 (s), –14.0 (s), –10.1 (s), –9.2 (s), 0.1 (s) (skeletal boron atoms), 67.5 (s, br, exopolyhedral boron atom) see Figure 12.

Method 2: Finely-cut alkali metal pieces were added to a solution of **2** (0.07 g, 0.14 mmol) in tetrahydrofuran (0.5 mL). A purple colour occurred immediately at the metal surface followed by a clear dark red solution after 2 h. The reaction mixture was then analysed by ^{11}B NMR spectroscopy and in many experiments the desired dianion was present as the only carborane compound.(Table S1) ^1H and ^{13}C NMR spectra were also obtained for Na_2[**2**] when deuterated THF was used in place of THF. Na_2[**2**]. $^1H\{^{11}B\}$ NMR (d_8-THF): δ [ppm] = 0.26 (s, 2 H, BH), 1.16 (s, 2 H, BH), 1.59 (s, 2 H, BH), 2.09 (s, 6 H, *para*-CH_3), 2.19 (s, 1 H, BH), 2.35 (s, 12 H, *ortho*-CH_3), 6.46 (s, 4 H, CH_{Mes}), 6.68 (t, 7.5 Hz, 1 H, H_{para}), 6.82 (apparent triplet, ~8 Hz, 2 H, H_{Ph} *meta*), 7.37 (d, 8 Hz, 2 H, H_{Ph} *ortho*); $^{13}C\{^1H\}$ NMR (d_8-THF): 21.3 (s, *para*-CH_3), 122.3 (s, CH_{Ph} *para*), 126.7 (s, CH_{Ph} *meta*), 127.7 (s, CH_{Mes}), 128.9 (s, CH_{Ph} *ortho*), 133.1 (s, C_{Mes}-*para*), 140.8 (s, C_{Mes}-*ortho*), 148.7 (s, C_{Mes}-*ipso*), 153.5 (s, C_{Ph} *ipso*); the peak corresponding to *ortho*-CH_3 groups is hidden within the d_8-THF peak and the peaks for the cage carbons were not detected above the noise levels, see Figures S7 and S8 for $^1H\{^{11}B\}$ and ^{13}C NMR spectra. Exposing the dark red solution containing Na_2[**2**] slowly to air gave a light yellow solution identified by NMR spectroscopy to contain only the starting material **2**. Method 2 was also used in the reductions of **3** with alkali metals (Li, Na, K) but with deuterated THF in all cases and NMR data of M_2[**2**] (M = Li, Na, K) are listed in Table S2.

Photophysical measurements

For all solution state measurements, samples were contained in quartz cuvettes of 10 × 10 mm (Hellma type 111-QS, suprasil, optical precision). Cyclohexane was used as received from commercial sources (p. a. quality), the other solvents were dried by standard methods prior to use. Concentrations varied from 20 to 100 μM in order to get analysable emission spectra due to the low quantum yields. Effects of the concentration on the shape of the observed emission spectra were excluded in this concentration range.. Solid samples were prepared by vacuum sublimation on quartz plates (35 × 10 × 1 mm) using standard Schlenk equipment and conditions. Each plate was laid in a 100 mL round bottom flask and a crystal of the sample

substance placed below it was sublimed. Absorption was measured with a UV/VIS double-beam spectrometer (Shimadzu UV-2550), using the solvent as a reference.

The output of a continuous Xe-lamp (75 W, LOT Oriel) was wavelength-separated by a first monochromator (Spectra Pro ARC-175, 1800 l/mm grating, Blaze 250 nm) and then used to irradiate a sample. The fluorescence was collected by mirror optics at right angles and imaged on the entrance slit of a second spectrometer while compensating astigmatism at the same time. The signal was detected by a back-thinned CCD camera (RoperScientific, 1024 \ 256 pixels) in the exit plane of the spectrometer. The resulting images were spatially and spectrally resolved. As the next step, one averaged fluorescence spectrum was calculated from the raw images and stored in the computer. This process was repeated for different excitation wavelengths. The result is a two-dimensional fluorescence pattern with the *y*-axis corresponding to the excitation, and the *x*-axis to the emission wavelength. The wavelength range is λ_{ex} = 230-430 nm (in 1 nm increments) for the UV light and λ_{em} = 305-894 nm for the detector. The time to acquire a complete EES is typically less than 15 min. Post-processing of the EES includes subtraction of the dark current background, conversion of pixel to wavelength scales, and multiplication with a reference file to take the varying lamp intensity as well as grating and detection efficiency into account. Stokes shifts were calculated from excitation and emission maxima, which were extracted from spectra that were converted from wavelength to wavenumbers beforehand. The quantum yields in solution were determined against POPOP (*p*-bis-5-phenyl-oxazolyl(2)-benzene) (Φ_F = 0.93) as the standard.

The solid-state fluorescence was measured by addition of an integrating sphere (Labsphere, coated with Spectralon, Ø 12.5 cm) to the existing experimental setup. At the exit slit of the first monochromator the exciting light was transferred into a quartz fibre (LOT Oriel, LLB592). It passed a condensor lens and illuminated a 1 cm^2 area on the sample in the centre of the sphere. The emission and exciting light was imaged by a second quartz fibre on the entrance slit of the detection monochromator. Post-processing of the spectra was done as described above. The measurement and calculation of quantum yields was performed according to the method described by Mello.[55]

Electrochemistry

Cyclic voltammetric measurements were carried out using an EcoChemie Autolab PG-STAT 30 potentiostat at 298 K with a platinum or glassy carbon working electrode and platinum

wires as counter and reference electrodes in a nitrogen-containing glove box with 0.1 M $^{n}Bu_4NPF_6$ in dichloromethane or acetonitrile. Scan rates of 100 mV s^{-1} and analyte concentrations of 10^{-3} M were used. The ferrocene/ferrocenium FcH/FcH^+ couple served as internal reference at 0.0 V for potential measurements and peak-peak separations of this couple were generally in the region of 90-110 mV.

Crystallographic studies

Single crystals were coated with a layer of hydrocarbon oil and attached to a glass fiber. Crystallographic data were collected with a Bruker AXS X8 Prospector Ultra APEX II diffractometer with Cu-Kα radiation (graphite monochromator, λ = 1.54178 Å) at 100 K. Crystallographic programs used for structure solution and refinement were from SHELX-97.[56] The structures were solved by direct methods and were refined by using full-matrix least squares on F^2 of all unique reflections with anisotropic thermal parameters for all non-hydrogen atoms. The hydrogen atoms bonded to the carborane units were refined isotropically, all other hydrogen atoms were refined using a riding model with U(H) = 1.5 U_{eq} for CH_3 groups and U(H) = 1.2 U_{eq} for all others. Crystallographic data for the compounds are listed in Table S3. CCDC-???? (**1**) and CCDC-???? (**2**), contain the supplementary crystallographic data for this paper. These data can be obtained free of charge from the Cambridge Crystallographic Data Centre via www.ccdc.cam.ac.uk/data_request/cif

Computational details

All computations were carried out with the Gaussian 09 package.[57] The model geometries were fully optimised with the B3LYP functional[58] with no symmetry constraints using the 6-31G* basis set[59] for all atoms. Frequency calculations on these optimised geometries (**7** and **8**) revealed no imaginary frequencies. Computed absorption data were obtained from TD-DFT[60] calculations on S_0 geometries whereas computed emission data were from the S_1 geometries. The MO diagrams and MO compositions were generated with the Molekel[61] and GaussSum[62] packages, respectively. Calculated ^{11}B and ^{13}C NMR chemical shifts obtained at the GIAO[63]-B3LYP/6-31G*//B3LYP/6-31G* level on the optimised geometries were referenced to $BF_3{\cdot}OEt_2$ for ^{11}B: δ (^{11}B) = 106.7 - σ(^{11}B) and referenced to TMS for ^{13}C: δ (^{13}C) = 189.4 - σ(^{13}C). Computed NMR values reported here were averaged where possible.

References

1. (a) C. D. Entwistle and T. B. Marder, *Angew. Chem*., 2002, **114**, 3051–3056, (*Angew. Chem., Int. Ed.*, 2002, **41**, 2927–2931); (b) C. D. Entwistle and T. B. Marder, *Chem. Mater.*, 2004, **16**, 4574–4585; (c) S. Yamaguchi and A. Wakamiya, *Pure Appl. Chem.*, 2006, **78**, 1413–1424; (d) F. Jäkle, *Coord. Chem. Rev.*, 2006, **250**, 1107–1121.

2. (a) T. Noda and Y. Shirota, *J. Am. Chem. Soc*., 1998, **120**, 9714-9715; (b) M. Kinoshita, N. Fujii, T. Tsukaki and Y. Shirota, *Synth. Met.*, 2001, **121**, 1571-1572.

3. (a) W.-L. Jia, D.-R. Bai, T.Mc Cormick, Q-D. Liu, M. Motala, R-Y. Wang, C. Seward, Y. Tao and S. Wang, *Chem. Eur. J.*, 2004, **10**, 994-1006; (b) W-L. Jia, D. Feng, D-R. Bai, Z.H. Lu, S. Wang and G. Vamvounis, *Chem. Mater*., 2005, **17**, 164-170; (c) M. Mazzeo, V. Vitale, F. Della Sala, M. Anni, G. Barbarella, L. Favaretto, G. Sotgui, R. Cingolani and G. Gigli, *Adv. Mater*., 2005, **17**, 34-39.

4. A. Schulz and W. Kaim, *Chem. Ber.*, 1989, **122**, 1863-1868.

5. M. E. Glogowski and J. L. R. Williams, *J. Organomet. Chem.*, 1981, **218**, 137-146.

6. (a) T. Noda, H. Ogawa and Y. Shirota*, Adv. Mater*., 1999, **11**, 283-285; (b) T. Noda and Y. Shirota, *J. Lumin*., 2000, **87-89**, 1168-1170; (c) Y. Shirota, M. Kinoshita, T. Noda, K. Okumuto and T. Ohara, *J. Am. Chem. Soc*., 2000, **122**, 11021-11022; (d) W.-Y. Wong, S.-Y. Poon, M.-F. Lin and W.-K. Wong, *Aust. J. Chem.*, 2007, **60**, 915-922; (e) G.-J. Zhou, G.-L. Ho, W.-Y. Wong, Q. Wang, D.-G. Ma, L.-X. Wang, Z.-Y. Lin, T.B. Marder and A. Beeby, *Adv. Funct. Mater*. 2008, **18**, 499-511; (f) C.-L. Ho; B. Yao, B. Zhang, K.-L. Wong, W.-Y. Wong, Z. Xie, L. Wang and Z. Lin, *J. Organomet. Chem.*, 2013, **730**, 144-155.

7. (a) E. Sakuda, A. Funahashi and N. Kitamura, *Inorg. Chem.*, 2006, **45**, 10670-10677; (b) M. Melaimi and F. P. Gabbaï, *J. Am. Chem. Soc.*, 2005, **127**, 9680-9681; (c) Y. Kim and F. P. Gabbaï, *J. Am. Chem. Soc.*, 2009, **131**, 3363-3369; (d) S.-B. Zhao, T. McCormick and S. Wang, *Inorg. Chem.*, 2007, **46**, 10965-10967; (e) M.-S. Yuan, Z.-Q. Liu and Q. Fang, *J. Org. Chem.*, 2007, **72**, 7915-7922; (f) X. Y. Liu, D. R. Bai and S. Wang, *Angew. Chem.*, 2006, **118**, 5601-5604; *Angew. Chem., Int. Ed.*, 2006, **45**, 5475-5478; (g) D.-R. Bai, X.-Y. Liu and S. Wang, *Chem. Eur. J.*, 2007, **13**, 5713-5723; (h) M. H. Lee, T. Agou, J. Kobayashi, T. Kawashima and F. P. Gabbaï, *Chem. Commun.*, 2007, 1133-1135; (i) T. W. Hudnall, M. Melaïmi and F. P. Gabbaï, *Org. Lett.*, 2006, **8**, 2747-2749; (j) H.-P. Shi, J.-X. Dai, L. Xu, L.-W. Shi, L. Fang, S.-M. Shuang and C. Dong, *Org. Biomol. Chem.*, 2012, **10**, 3852-3858; (k) C.-W. Chiu and F. P. Gabbaï, *J. Am. Chem. Soc.*, 2006, **128**, 14248-14249; (l) S. Yamaguchi, S. Akiyama and K.

Tamao, *J. Am. Chem. Soc.*, 2001, **123**, 11372-11375; (m) S. Yamaguchi, T. Shirasaka, S. Akiyama and K. Tamao, *J. Am. Chem. Soc.*, 2002, **124**, 8816-8817; (n) Y. Kubo, M. Yamamoto, M. Ikeda, M. Takeuchi, S. Shinkai, S. Yamaguchi and K. Tamao, *Angew. Chem.*, 2003, **115**, 2082-2086; *Angew. Chem. Int. Ed.*, 2003, **42**, 2036-2040; (o) S. Solé and F. P. Gabbaï, *Chem. Commun.*, 2004, 1284-1285; (p) T. W. Hudnall and F. P. Gabbaï, *J. Am. Chem. Soc*., *2007*, 129, 11978-11986. (q) A. Sundararaman, M. Victor, R. Varughese and F. Jäkle, *J. Am. Chem. Soc.*, 2005, **127**, 13748-13749; (r) K. Parab, K. Venkatasubbaiah and F. Jäkle, *J. Am. Chem. Soc.,* 2006, **128**, 12879-12885; (s) L. Weber, D. Eickhoff, J. Kahlert, L. Böhling, A. Brockhinke, H.-G. Stammler, B. Neumann and M. A. Fox, *Dalton Trans.*, 2012, **41**, 10328-10346; (t) W.-J. Xu, S.-H. Liu, X. Zhao, N. Zhao, X.-Q. Yu and W. Huang, *Chem. Eur. J.*, 2013, **19**, 621-629.

8. (a) Y. Kim, H.-S. Huh, M. H. Lee, I. L. Lenov, H. Zhao and F. P. Gabbaï, *Chem. Eur. J.*, 2011, **17**, 2057-2062; (b) C. Wang, J. Jia, W.-N. Zhang, H.-Y. Zhang and C.H. Zhao, *Chem. Eur. J.*, 2014, **17**, 16590-16601.
9. R. N. Grimes, *Carboranes*, Academic Press (Elsevier), New York, 2nd edn, 2011.
10. For other reviews on carboranes see (a) B. P. Dash, R. Satapathy, J. A. Maguire and N. S. Hosmane, *New J. Chem.*, 2011, **35**, 1955-1972; (b) I. B. Sivaev and V. V. Bregadze, *Eur. J. Inorg. Chem.*, 2009, 1433-1450; (c) F. Issa, M. Kassiou and L. M. Rendina, *Chem. Rev.*, 2011, **111**, 5701-5722; (d) M. Scholz and E. Hey-Hawkins, *Chem. Rev.*, 2011, **111**, 7035-7062; (e) J. F. Valliant, K. J. Guenther, A. S. King, P. Morel, P. Schaffer, O. O. Sogbein and K. A. Stephenson, *Coord. Chem. Rev.*, 2002, **232**, 173-230; (f) V. N. Kalinin and V. A. Ol'shevskaya, *Russ. Chem. Bull.*, 2008, **57**, 815-836; (g) V. I. Bregadze, *Chem. Rev.*, 1992, **92**, 209-223; (h) A. F. Armstrong and J. F. Valliant, *Dalton Trans.*, 2007, 4240-4251; (i) L. A. Leites, *Chem. Rev.*, 1992, **92**, 279-323; (j) T. J. Wedge and M. F. Hawthorne, *Coord. Chem. Rev.*, 2003, **240**, 111-128; (k) D. Olid, C. Viñas and F. Teixidor, *Chem. Soc. Rev.*, 2013, **42**, 3318-3336; (l) C. Viñas, R. Núñez and F. Teixidor, '*Large molecules containing icosahedral boron clusters designed for potential applications*', Chapter 27 in Boron Science, N.S. Hosmane, CRC Press, New York, 2012.
11. (a) B. P. Dash, R. Satapathy, J. A. Maguire and N. S. Hosmane, *Chem. Commun.*, 2009, 3267-3269; (b) Yu. A. Kabachii and P. M. Valetskii, *Int. J. Polym. Mater.*, 1990, **14**, 9-19; (c) K. Hideaki, O. Koichi, I. Motokuni, S. Toshiya, K. Shigeki and A. Isao, *Chem. Mater.*, 2003, **15**, 355-362; (d) E. Hao, B. Fabre, F. R. Fronczek and M. G. H. Vicente,

Chem. Commun., 2007, 4387-4389; (e) E. Hao, B. Fabre, F. R. Fronczek and M. G. H. Vicente, *Chem. Mater.*, 2007, **19**, 6195–6205; (f) M. A. Fox and K. Wade, *J. Mater. Chem.*, 2002, **12**, 1301–1306; (g) O. K. Farha, A. M. Spokoyny, K. L. Mulfort, M. F. Hawthorne, C. A. Mirkin and J. T. Hupp, *J. Am. Chem. Soc.*, 2007, **129**, 12680–12681.

12. (a) J. Llop, C. Viñas, J. M. Oliva, F. Teixidor, M. A. Flores, R. Kivekäs and R. Sillanpää, *J. Organomet. Chem.*, 2002, **657**, 232-238; (b) J. M. Oliva, N. L. Allan, P. v. R. Schleyer, C. Viñas and F. Teixidor, *J. Am. Chem. Soc.*, 2005, **127**, 13538-13547; (c) D. A. Brown, W. Clegg, H. M. Colquhoun, J. A. Daniels, I. R. Stephenson and K. Wade, *J. Chem. Soc., Chem. Commun.*, 1987, 889-891; (d) L. A. Boyd, W. Clegg, R. C. B. Copley, M. G. Davidson, M. A. Fox, T. G. Hibbert, J. A. K. Howard, A. Mackinnon, R. J. Peace and K. Wade, *Dalton Trans.*, 2004, 2786-2799.
13. (a) T. D. Getman, C. B. Knobler and M. F. Hawthorne, *J. Am. Chem. Soc.*, 1990, **112**, 4593-4594; (b) T. D. Getman, C. B. Knobler and M. F. Hawthorne, *Inorg. Chem.*, 1992, **31**, 101-105.
14. (a) V. Z. Paschenko, R. P. Evstigneeva, V. V. Gorokhov, V. N. Luzgina, V. B. Tusov and A. B. Rubin, *J. Photochem. Photobiol. B: Biol.*, 2000, **54**, 162-167; (b) V. N. Luzgina, V. A. Ol'shevskaya, A. V. Sekridova, A. F. Mironov, V. N. Kalinin, V. Z. Pashchenko, V. V. Gorokhov, V. B. Tusov and A. A. Shtil', *Russ. J. Org. Chem.*, 2007, **43**, 1243-1251; (c) B.P. Dash, R. Satapathy, E.R. Galliard, K.M. Norton, J.A. Maguire, N. Chug and N.S. Hosmane, *Inorg. Chem.*, 2011, **50**, 5485-5493; (d) A. Ferrer-Ugalde, E. J. Juárez-Pérez, F. Teixidor, C. Viñas, R. Sillanpää, E. Pérez-Inestrosa and R. Núñez, *Chem. Eur. J.*, 2012, **18**, 544-553; (e) L. Zhu, W. Lv, S. Liu, H. Yan, Q. Zhao and W. Huang, *Chem. Commun*., 2013, **49**, 10638-10640; (f) A. Ferrer-Ugalde, A. González-Campo, C. Viñas, J. Rodriguez-Romero, R. Santillan, N. Farfán, R. Sillanpää, A. Sousa-Pedrares, R. Núñez and F. Teixidor, *Chem. Eur. J.*, 2014, **20**, 9940-9951; (g) G.F. Jin, Y.-J. Cho, K.-R. Wee, S.A. Hong, I.-H. Suh, H.-J. Son, J.-D. Lee, W.-S. Han, D.W. Cho and S.O. Kang, *Dalton Trans*., 2015, DOI: 10.1039/C4DT03123G.
15. (a) K. Kokado and Y. Chujo, *Macromolecules*, 2009, **42**, 1418-1420; (b) K. Kokado, Y. Tokoro and Y. Chujo, *Macromolecules*, 2009, **42**, 9238-9242; (c) K. Kokado, A. Nagai and Y. Chujo, *Macromolecules*, 2010, **43**, 6463-6468; (d) K. Kokado and Y. Chujo, *Polym. J.*, 2010, **42**, 363-367; (e) K. Kokado, A. Nagai and Y. Chujo, *Tetrahedron Lett.*, 2011, **52**, 293-296; (f) K. Kokado and Y. Chujo, *Dalton Trans.*, 2011, **40**, 1919-1923; (g) K. Kokado and Y. Chujo, *J. Org. Chem.*, 2011, **76**, 316-319; (h) M. Tominaga, H.

Naito, Y. Morisaki and Y. Chujo, *Asian J. Org. Chem*., 2014, **3**, 624-631; (i) M. Tominaga, H. Naito, Y. Morisaki and Y. Chujo, *New J. Chem*., 2014, **38**, 5686-5690.

16. (a) K.-R. Wee, W.-S. Han, D. W. Cho, S. Kwon, C. Pac and S. O. Kang, *Angew. Chem.*, 2012, **124**, 2731-2734; *Angew. Chem., Int. Ed.*, 2012, **51**, 2677-2680; (b) S. Kwon, K.-R. Wee, Y.-J. Cho and S.O. Kang, *Chem. Eur. J*., 2014, **20**, 5953-5960.
17. S. Inagi, K. Hosoi, T. Kubo, N. Shida and T. Fuchigami, *Electrochemistry*, 2013, **81**, 368-370.
18. (a) M. Eo, M.H. Park, T. Kim, Y. Do and M.H. Lee, *Polymer*, 2013, **54**, 6321-6328; (b) H.J. Bae, H. Kim, K.M. Lee, T. Kim, Y.S. Lee, Y. Do and M.H. Lee, *Dalton Trans.*, 2014, **43**, 4978-4985.
19. (a) A. R. Davis, J. J. Peterson and K. R. Carter, *ACS Macro Lett.*, 2012, **1**, 469-472; (b) J. J. Peterson, A. R. Davis, M. Werre, E. B. Coughlin and K. R. Carter, *ACS Appl. Mater. Interfaces*, 2011, **3**, 1796-1799; (c) J. J. Peterson, M. Werre, Y. C. Simon, E. B. Coughlin and K. R. Carter, *Macromolecules*, 2009, **42**, 8594-8598.
20. L. Weber, J. Kahlert, R. Brockhinke, L. Böhling, A. Brockhinke, H.-G. Stammler, B. Neumann, R. A. Harder and M. A. Fox, *Chem. Eur. J.*, 2012, **18**, 8347-8357.
21. L. Weber, J. Kahlert, L. Böhling, A. Brockhinke, H.-G. Stammler, B. Neumann, R. A. Harder, P. J. Low and M. A. Fox, *Dalton Trans.*, 2013, **42**, 2266-2281.
22. L. Weber, J. Kahlert, R. Brockhinke, L. Böhling, J. Halama, A. Brockhinke, H.-G. Stammler, B. Neumann, C. Nervi, R. A. Harder, M. A. Fox, *Dalton Trans.*, 2013, **42**, 10982-10996.
23. K.-R. Wee, Y.-J. Cho, J. K. Song and S. O. Kang, *Angew. Chem.*, 2013, **125**, 9864-9867; *Angew. Chem., Int. Ed.*, 2013, **52**, 9682-9685.
24. K.-R. Wee, Y.-J. Cho, S. Jeong, S. Kwon, J.-D. Lee, I.-H. Suh and S.O. Kang, *J. Am. Chem. Soc.*, 2012, **134**, 17982-17990.
25. (a) J. O. Huh, H. Kim, K. M. Lee, Y. S. Lee, Y. Do and M. H. Lee, *Chem. Commun.*, 2010, **46**, 1138-1140; (b) K.M. Lee, J.O. Huh, T. Kim, Y. Do and M.H. Lee, *Dalton Trans.*, 2011, **40**, 11758-11764; (c) K. C. Song, H. Kim, K. M. Lee, Y. S. Lee, Y. Do and M. H. Lee, *Dalton Trans.*, 2013, **42**, 2351-2354.
26. (a) C. Malan and C. Morin, *Tetrahedron Lett.*, 1997, **38**, 6599-6602; (b) D. A. Brown, H. M. Colquhoun, J. A. Daniels, J. A. H. MacBride, I. R. Stephenson and K. Wade, *J. Mater. Chem.* 1992, **2**, 793-804; (c) Y. Z. Voloshin, S. Y. Erdyakov, I. G. Makarenko, E. G. Lebed', T. V. Potapova, S. V. Svidlov, Z. A. Starikova, E. V. Pol'shin, M. E.

Gurskii and Y. N. Bubnov, *Russ. Chem. Bull.*, 2007, **56**, 1787-1794; (d) G. Zi, H.-W. Li and Z. Xie, *Organometallics*, 2002, **21**, 3850-3855; (e) S. Y. Erdyakov, Y. Z. Voloshin, I. G. Makarenko, E. G. Lebed, T. V. Potapova, A. V. Ignatenko, A. V. Vologzhanina, M. E. Gurskii and Y. N. Bubnov, *Inorg. Chem. Commun.*, 2009, **12**, 135-139; (f) J. L. Boone, R. J. Brotherton and L. L. Petterson, *Inorg. Chem.* 1965, **4**, 910-912.

27. (a) G. Zi, H.-W. Li and Z. Xie, *Organometallics*, 2002, **21**, 1136-1145; (b) Y. Nie, J. Miao, H. Wadepohl, H. Pritzkow, T. Oeser and W. Siebert, *Z. Anorg. Allg. Chem.*, 2013, **639**, 1188-1193.
28. Y. Nie, J. Miao, H. Pritzkow, H. Wadepohl and W. Siebert, *J. Organomet. Chem.*, 2013, **747**, 174-177.
29. N. M. D. Brown, F. Davidson, R. McMullan and J. W. Wilson, *J. Org. Chem.*, 1980, **193**, 271-282.
30. Z. G. Lewis and A. J. Welch, *Acta Crystallogr., Sect. C: Cryst. Struct. Commun.*, 1993, **49**, 705-710.
31. A search in the CCDC database in May 2012 revealed that 95% of the B-C_{Mes} bond lengths in 37 structures of *p*-substituted dimesitylborylbenzene derivatives are in the range of 1.55 Å - 1.61 Å. The interplanar angles between the mesityl rings and the planes defined by the boryl-boron atom and the three neighbouring carbon atoms were found between 42.9° and 67.5° in these structures.
32. (a) T. D. McGrath and A. J. Welch, *Acta Crystallogr., Sect. C: Cryst. Struct. Commun.*, 1995, **51**, 646-649; (b) E. S. Alekseyeva, M. A. Fox, J. A. K. Howard, J. A. H. MacBride and K. Wade, *Appl. Organometal. Chem.*, 2003, **17**, 499-508.
33. L. Weber, D. Eickhoff, T.B. Marder, M.A. Fox, P.J. Low, A.D. Dwyer, D.J. Tozer, S. Schwedler, A. Brockhinke, H.-G. Stammler and B. Neumann, *Chem. Eur. J.*, 2012, **18**, 1369-1382.
34. (a) M. V. Yarosh, T. V. Baranova, V. L. Shirokii, A. A. Érdman and N. A. Maier, *Élektrokhimiya*, 1993, **29**, 921-922 (Russian; English version *Russ. J. Electrochem.*, 1993, **29**, 789-790); (b) M. V. Yarosh, T. V. Baranova, V. L. Shirokii, A. A. Érdman and N. A. Maier, *Élektrokhimiya*, 1994, **30**, 406-408 (Russian; English version *Russ. J. Electrochem.*, 1994, **30**, 366-368).
35. R.A. Harder, J.A.H. MacBride, G.P. Rivers, D.S. Yufit, A.E. Goeta, J.A.K. Howard, K. Wade and M.A. Fox, *Tetrahedron*, 2014, **70**, 5182-5189.
36. M. A. Fox, C. Nervi, A. Crivello and P. J. Low, *Chem. Commun.*, 2007, 2372-2374.

37. H. Tricas, M. Colon, D. Ellis, S. A. Macgregor, D. McKay, G. M. Rosair, A. J. Welch, I. V. Glukhov, F. Rossi, F. Laschi and P. Zanello, *Dalton Trans.*, 2011, **40**, 4200-4211.

38. (a) M. A. Fox, C. Nervi, A. Crivello, A. S. Batsanov, J. A. K. Howard, K. Wade and P. J. Low, *J. Solid State Electrochem.*, 2009, **13**, 1483-1495; (b) G.F. Jin, J.-H. Hwang, J.-D. Lee, K.-R. Wee, I.-H. Suh and S.O. Kang, *Chem. Commun.*, 2013, **49**, 9398-9400; (c) J. Kahlert, H.-G. Stammler, B. Neumann, R.A. Harder, L. Weber and M.A. Fox, *Angew. Chem.* 2014, **126**, 3776-3779; *Angew. Chem. Int. Ed.*, 2014, **53**, 3702-3705.

39. K. Hosoi, S. Inagi, T. Kubo and T. Fuchigami, *Chem. Commun.*, 2011, **47**, 8632-8634.

40. (a) A.V. Lebedev, A.V. Buchtiarov, N.N. Golyshin, Y.G. Kudryatsev, I.Y. Lovchinovsky and L.N. Rozhkov, *Organomet. Chem. USSR,* 1991, **4**, 205-208 (English Transl.); (b) A.V. Lebedev, A.V. Bukhtiarov, Y.G. Kudryavtev and I.N. Rozhkov, *Organomet. Chem. USSR*, 1991, **4**, 208-212 (English Transl.); (c) A.V. Bukhtiarov, V.N. Golyshin, A.V. Lebedev, Y.G. Kudryavtsev, I.A. Rodnikov, L.I. Zakharkin and O.V. Kuz'min, *Dokl. Acad. Sci. USSR*, 1989, 45-48 (English Transl.).

41. M.A. Fox, '*Polyhedral Carboranes*', Chapter 3.02 in Comprehensive Organometallic Chemistry III, R.H. Crabtree, D.M.P. Mingos, Elsevier, Oxford, 2007.

42. K. Chui, H.-W. Li and Z. Xie, *Organometallics*, 2000, **19**, 5447-5453.

43. (a) G. Zi, H.-W. Li and Z. Xie, *Organometallics*, 2001, **20**, 3836-3838; (b) G. Zi, H.-W. Li and Z. Xie, *Chem. Commun.*, 2001, 1110-1111.

44. G. Zi, H.-W. Li and Z. Xie, *Organometallics*, 2002, **21**, 5415-5427.

45. (a) M.-S. Cheung, H.-S. Chan and Z. Xie, *Organometallics*, 2004, **23**, 517-526; (b) H. Shen, H.-S. Chan and Z. Xie, *Organometallics*, 2006, **25**, 2617-2625; (c) L. Deng, H.-S. Chan and Z. Xie, *Inorg. Chem*., 2007, **46**, 2716-2724.

46. L. Deng, M.-S. Cheung, H.-S. Chen and Z. Xie, *Organometallics*, 2005, **24**, 6244-6249.

47. (a) T.L. Venable, R.B. Maynard and R.N. Grimes, *J. Am. Chem. Soc.*, 1984, **106**, 6187-6193; (b) J.T. Spencer, M.R. Pourian, R.J. Butcher, E. Sinn and R.N. Grimes, *Organometallics*, 1987, **6**, 335-343; (c) N.S. Hosmane, T.J. Colacot, H. Zhang, J. Yang, J.A. Maguire, Y. Wang, M.B. Ezhova, A. Franken, T. Demissie, K.-J. Lu, D. Zhu, J.L.C. Thomas, J.D. Collins, T.G. Gray, S.N. Hosmane and W.N. Lipscomb, *Organometallics*, 1998, **17**, 5294-5309.

48. J. P. H. Charmant, M. F. Haddow, R. Mistry, N. C. Norman, A. G. Orpen and P. G. Pringle, *Dalton Trans.*, 2008, 1409-1411.

49. (a) M. Bühl and P. v. R. Schleyer, *J. Am. Chem. Soc.* 1992, **114**, 477-491; (b) P. v. R. Schleyer, J. Gauss, M. Bühl, R. Greatrex and M. A. Fox, *J. Chem. Soc. Chem. Commun.* 1993, 1766-1768; (c) C. E. Willans, C. A. Kilner and M. A. Fox, *Chem. Eur. J.* 2010, **16**, 10644-10648.

50. S. Zlatogorsky, D. Ellis, G.M. Rosair and A.J. Welch, *Chem. Commun.*, 2007, 2178-2180.

51. J. Zhang, X. Fu, Z. Lin and Z. Xie, *Inorg. Chem.*, 2015, in press **DOI:** 10.1021/ic502866h.

52. (a) L.I. Zakharkin, V.N. Kalinin and L.S. Podvisotskaya, *Bull. Acad. Sci. USSR, Div. Chem. Sci.*, 1966, 1444 (English Transl.); (b) L.I. Zakharkin, V.N. Kalinin and L.S. Podvisotskaya, *Bull. Acad. Sci. USSR, Div. Chem. Sci.*, 1967, 2212-2217 (English Transl.); (c) L.I. Zakharkin, *Pure Appl. Chem.*, 1972, **29**, 513-526; (d) L.I. Zakharkin, V.N. Kalinin, V.A. Antonovich and E.G. Rhys, *Bull. Acad. Sci. USSR, Div. Chem. Sci.*, 1976, 1009-1014 (English Transl.).

53. A. Pelter, K. Smith and H. C. Brown, *Borane Reagents* Academic Press London, 1988, p. 428.

54. L. I. Zakharkin, V. I. Bregadze and O. Y. Okhlobystin, *J. Organomet. Chem.*, 1966, **6**, 228-234.

55. J. C. de Mello, H. F. Wittmann and R. H. Friend, *Adv. Mater.*, 1997, **9**, 230-232.

56. G. M. Sheldrick, *Acta Cryst.,* 2008, **A64**, 112-122.

57. Gaussian 09, Revision A.02, M. J. Frisch, G. W. Trucks, H. B. Schlegel, G. E. Scuseria, M. A. Robb, J. R. Cheeseman, G. Scalmani, V. Barone, B. Mennucci, G. A. Petersson, H. Nakatsuji, M. Caricato, X. Li, H. P. Hratchian, A. F. Izmaylov, J. Bloino, G. Zheng, J. L. Sonnenberg, M. Hada, M. Ehara, K. Toyota, R. Fukuda, J. Hasegawa, M. Ishida, T. Nakajima, Y. Honda, O. Kitao, H. Nakai, T. Vreven, Jr., J. A. Montgomery, J. E. Peralta, F. Ogliaro, M. Bearpark, J. J. Heyd, E. Brothers, K. N. Kudin, V. N. Staroverov, R. Kobayashi, J. Normand, K. Raghavachari, A. Rendell, J. C. Burant, S. S. Iyengar, J. Tomasi, M. Cossi, N. Rega, J. M. Millam, M. Klene, J. E. Knox, J. B. Cross, V. Bakken, C. Adamo, J. Jaramillo, R. Gomperts, R. E. Stratmann, O. Yazyev, A. J. Austin, R. Cammi, C. Pomelli, J. W. Ochterski, R. L. Martin, K. Morokuma, V. G. Zakrzewski, G. A. Voth, P. Salvador, J. J. Dannenberg, S. Dapprich, A. D. Daniels, O. Farkas, J. B. Foresman, J. V. Ortiz, J. Cioslowski and D. J. Fox, *Gaussian, Inc.*, Wallingford CT, **2009**.

58. (a) A. D. Becke, *J. Chem. Phys.*, 1993, **98**, 5648-5652; (b) C. Lee, W. Yang and R. G. Parr, *Phys. Rev. B*, 1988, **37**, 785-789.

59. (a) G. A. Petersson and M. A. Al-Laham, *J. Chem. Phys.*, 1991, **94**, 6081-6090; (b) G. A. Petersson, A. Bennett, T. G. Tensfeldt, M. A. Al-Laham, W. A. Shirley and J. Mantzaris, *J. Chem. Phys.*, 1988, **89**, 2193-2218.

60. E. Runge and E. K. U. Gross, *Phys. Rev. Lett.*, 1984, **52**, 997-1000.

61. U. Varetto, *MOLEKEL Version*, Swiss National Supercomputing Centre, Mann, Switzerland.

62. N. M. O'Boyle, A. L. Tenderholt and K. M. Langner, *J. Comp. Chem*., 2008, **29**, 839-845.

63. (a) R. Ditchfield, *Mol. Phys.*, 1974, **27**, 789-807; (b) C.M. Rohling, L.C. Allen and R. Ditchfield, *Chem. Phys.*, 1984, **87**, 9-15; (c) K. Wolinski, J. F. Hinton and P. Pulay, *J. Am. Chem. Soc*., 1990, **112**, 8251-8260.